

Bounds on the neutrino mixing angles and CP phase for an $SO(10)$ model with lopsided mass matrices

Carl H. Albright*

*Department of Physics, Northern Illinois University, DeKalb, IL 60115 and
Fermi National Accelerator Laboratory, P.O. Box 500, Batavia, IL 60510*

Abstract

The bounds on the neutrino mixing angles and CP Dirac phase for an $SO(10)$ model with lopsided mass matrices, arising from the presence of $\mathbf{16}_H$ and $\overline{\mathbf{16}}_H$ Higgs representations, are studied by variation of the one real and three unknown complex input parameters for the right-handed Majorana neutrino mass matrix. The scatter plots obtained favor nearly maximal atmospheric neutrino mixing, while the reactor neutrino mixing lies in the range $10^{-5} \lesssim \sin^2 \theta_{13} \lesssim 1 \times 10^{-2}$ with values greater than 10^{-3} most densely populated. A rather compelling scenario within the model follows, if we restrict the three unknown complex parameters to their imaginary axes and set two of them equal. We then find the scatter plots are reduced to narrow bands, as the mixing angles and CP phase become highly correlated and predictive. The bounds on the mixing angles and phase then become $0.45 \lesssim \sin^2 \theta_{23} \lesssim 0.55$, $0.38 \lesssim \tan^2 \theta_{12} \lesssim 0.50$, $0.002 \lesssim \sin^2 \theta_{13} \lesssim 0.003$, and $60^\circ \lesssim \pm \delta_{CP} \lesssim 85^\circ$. Moreover, successful leptogenesis and subsequent baryogenesis are also obtained, with η_B increasing from $(2.7 \text{ to } 6.3) \times 10^{-10}$ as $\sin^2 \theta_{23}$ increases from 0.45 to 0.55.

PACS numbers: 14.60.Pq, 12.10.Dm, 12.15.Ff, 12.60.Jv

*Electronic address: albright@fnal.gov

I. INTRODUCTION

Since the discovery of atmospheric neutrino oscillations [1], more recently that of solar neutrino oscillations [2], and still more recently confirmation of these two types of neutrino oscillations with accelerator- and reactor-produced neutrinos [3, 4], many models have been proposed in the literature to explain the mass and mixing parameters associated with these oscillations [5]. (We have cited just the most recent references for those experiments and several review articles for the models proposed.) Some models restrict their scope to the lepton sector, while others such as grand unified models are more ambitious and attempt to explain the masses and mixings in both the lepton and quark sectors. The textures for the mass matrices obtained in the models may be simply postulated at the outset, derived from the observed mixing matrix with a diagonal charged lepton mass matrix, obtained from a certain unification group in conjunction with a well-defined family symmetry, or rely solely on the Clebsch-Gordon coefficients of that group.

Until now, all viable models for the lepton sector have only had to explain the apparent near maximal θ_{23} mixing angle for the atmospheric neutrinos and the less than maximal θ_{12} large mixing angle (LMA) solution for the solar neutrinos, while satisfying the two observed mass squared differences, Δm_{32}^2 and Δm_{21}^2 , and the upper bound for the still unobserved θ_{13} mixing angle. On the other hand, the neutrino mass hierarchy (normal or inverted), the Majorana vs Dirac nature of the neutrinos, the appropriate values for θ_{13} and the CP-violating phases (one Dirac and two Majorana) remain undetermined experimentally.

With the next more precise round of neutrino oscillation experiments which will restrict some of the unknowns, many of the more quantitative models proposed are not expected to survive the more stringent tests of their predictions. In particular, determination of the neutrino mass hierarchy will eliminate models based on an approximately conserved $L_e - L_\mu - L_\tau$ lepton number [6] if the hierarchy is observed to be normal, while the conventional type I seesaw models will be strongly disfavored if the hierarchy is observed to be inverted [7]. Moreover, small as opposed to very small predictions for θ_{13} pose a critical test for many models. It is thus of utmost importance to sharpen the predictions for each model, so that the list of presently viable models can be winnowed down as much as possible when the new data is obtained.

One particularly interesting class of models is that based on the $SO(10)$ grand unification

group. There are two kinds of minimal models in this class: those based on Higgs representations with dimensions **10**, **126**, $\overline{\mathbf{126}}$, and possibly also **120** and/or **210** [8]; and those based on **10**, **16**, $\overline{\mathbf{16}}$, and **45** representations [9]. The former type generally has symmetric and/or antisymmetric matrix elements, while the latter type generally involve lopsided matrices for the down quarks and charged leptons. The matrix textures are derived either from the Clebsch-Gordon coefficients required or from some Abelian or non-Abelian family symmetry. These two types of $SO(10)$ models tend to predict θ_{13} angles either near the present upper CHOOZ bound of 12° , or in the $1^\circ - 3^\circ$ range, respectively.

The purpose of this paper is to sharpen the allowed values for the mixing parameters of the lopsided $SO(10)$ model proposed some time ago by Babu, Barr, and the author [10]. Upon further refinement by the latter two authors [11], the model has become very predictive with all four quark mixing parameters and nine quark and charged lepton masses determined by just eight of the twelve model input parameters. The four remaining input parameters characterize the right-handed Majorana mass matrix with three of them complex in general. In most of the previous papers based on this model, the authors took the latter parameters to be real and adjusted them to give good fits to the then known neutrino mass and mixing data. Here we allow all three to be complex and obtain scatter plots of the predicted neutrino mixing parameters. In so doing, we obtain some bounds on θ_{13} and θ_{23} which, if violated, will rule out the model which has been highly successful to date. By introducing two very small additional parameters in the Dirac neutrino mass matrix, we find that the observed baryon asymmetry can be obtained through resonant leptogenesis in the model. In order to obtain the latter predictions, the bounds obtained on the neutrino mixing parameters and CP phase are even more tightly constrained. With maximal CP violation in the Majorana mass matrix and two of the three parameters equal, the mixing angles and phase become highly correlated with each other and the baryon asymmetry generated in the model.

In Sec. II we briefly review some of the model details and present the results of the parameter searches in Sec. III. A summary of the constraints found in the model is presented in Sec. IV, where we also briefly comment on the predictions of the model found by Jankowski and Marbury [12] for the $\mu \rightarrow e + \gamma$ lepton flavor-changing branching ratio. Their prediction is also crucial for the viability of the model and has a chance of being tested by the MEG collaboration [13] even before the values of the mixing angles are further restricted by new reactor and/or long baseline experiments.

II. $SO(10)$ MODEL AND ITS ARBITRARY PARAMETERS

The $SO(10)$ grand unified model as initially proposed by Babu, Barr and the author [10], and later updated by Barr and the author to apply to the large mixing angle (LMA) neutrino oscillation solution has already been described in great detail in the literature [11]. Here we just summarize the salient features and refer the reader to those references for more information.

The model is based on the minimum set of Higgs fields which solves the doublet-triplet splitting problem as proposed by Barr and Raby [14]. This requires just one $\mathbf{45}_H$ whose vacuum expectation value (VEV) points in the $B - L$ direction, two pairs of $\mathbf{16}_H$, $\overline{\mathbf{16}}_H$'s which stabilize the solution, along with several Higgs fields in the $\mathbf{10}_H$ representations and Higgs singlets. The Higgs superpotential exhibits the $U(1) \times Z_2 \times Z_2$ symmetry which is used for the flavor symmetry of the grand unified model. The combination of VEVs, $\langle \mathbf{45}_H \rangle_{B-L}$, $\langle \mathbf{16}_H \rangle$ and $\langle \overline{\mathbf{16}}_H \rangle$ break $SO(10)$ to the Standard Model, where the latter two VEVs point in the $SU(5)$ singlet direction. The electroweak VEVs arise from doublets in the $\mathbf{5}$ and $\overline{\mathbf{5}}$ representations of $SU(5)$ in the combinations

$$\begin{aligned} \langle H_u \rangle &= \langle \mathbf{5}(\mathbf{10}_H) \rangle, \\ \langle H_d \rangle &= \langle \overline{\mathbf{5}}(\mathbf{10}_H) \rangle \cos \gamma + \langle \overline{\mathbf{5}}(\mathbf{16}'_H) \rangle \sin \gamma, \end{aligned} \tag{1}$$

while the mixing orthogonal to H_d gets massive at the grand unified theory (GUT) scale. Matter superfields appear in three chiral $\mathbf{16}$'s, two pairs of vectorlike $\mathbf{16}$ and $\overline{\mathbf{16}}$, two $\mathbf{10}$'s and several $\mathbf{1}$'s. The mass matrices follow from Froggatt-Nielsen diagrams [15] in which the superheavy fields are integrated out, with the flavor symmetry allowing only certain particular contributions to their mass matrix elements. The Dirac mass matrices for the up quarks, down quarks, neutrinos and charged leptons are found to be

$$\begin{aligned} M_U &= \begin{pmatrix} \eta & \delta_N & \delta'_N \\ \delta_N & 0 & -\epsilon/3 \\ \delta'_N & \epsilon/3 & 1 \end{pmatrix} m_U, & M_D &= \begin{pmatrix} 0 & \delta & \delta' e^{i\phi} \\ \delta & 0 & -\epsilon/3 \\ \delta' e^{i\phi} & \sigma + \epsilon/3 & 1 \end{pmatrix} m_D, \\ M_N &= \begin{pmatrix} \eta & \delta_N & \delta'_N \\ \delta_N & 0 & \epsilon \\ \delta'_N & -\epsilon & 1 \end{pmatrix} m_U, & M_L &= \begin{pmatrix} 0 & \delta & \delta' e^{i\phi} \\ \delta & 0 & \sigma + \epsilon \\ \delta' e^{i\phi} & -\epsilon & 1 \end{pmatrix} m_D. \end{aligned} \tag{2}$$

in the convention where the left-handed fields label the rows and the left-handed conjugate

fields label the columns.

The entries in the first row and first column are the most uncertain, especially for the up quark and Dirac neutrino mass matrices, for they arise from higher order terms involving several integrations out of the massive neutrino lines. As originally proposed, the parameters δ_N and δ'_N were absent. In a later application of the model to leptogenesis [16], we have observed that the baryon asymmetry lies closer to the preferred value of $\eta_B \simeq 6.2 \times 10^{-10}$ [17], if we allow δ_N and δ'_N to take on nonzero values in the Dirac neutrino matrix M_N , which are small enough in M_U , however, so as not to upset the good results in the quark sector. We shall consider both possibilities for these two parameters in the searches to be presented.

The lopsided nature of the down quark and charged lepton mass matrices arises from the dominance of the $\sigma \mathbf{16}'_H$ contribution to the electroweak symmetry breaking over that of the $\mathbf{10}_H$. The pronounced lopsidedness with $\tan \beta \simeq 5$ readily explains the small V_{cb} quark mixing and near maximal $U_{\mu 3}$ atmospheric neutrino mixing for any reasonable right-handed Majorana neutrino mass matrix, M_R . All nine quark and charged lepton masses, plus the three CKM angles and CP phase, are well-fitted with the original eight input parameters defined at the GUT scale to fit the low scale observables after evolution downward from $\Lambda_{GUT} \simeq 2 \times 10^{16}$ GeV [18]:

$$\begin{aligned}
m_U &\simeq 113 \text{ GeV}, & m_D &\simeq 1 \text{ GeV}, \\
\sigma &= 1.83, & \epsilon &= 0.147, \\
\delta &= 0.00946, & \delta' &= 0.00827, \\
\phi &= 119.4^\circ, & \eta &= 6 \times 10^{-6},
\end{aligned} \tag{3}$$

The effective light neutrino mass matrix, M_ν , is obtained from the conventional type I seesaw mechanism [19] once the right-handed Majorana mass matrix, M_R , is specified. While the large atmospheric neutrino mixing $\nu_\mu \leftrightarrow \nu_\tau$ arises primarily from the structure of the charged lepton mass matrix M_L , the structure of the right-handed Majorana mass matrix M_R determines the type of $\nu_e \leftrightarrow \nu_\mu$, ν_τ solar neutrino mixing, so that the solar and atmospheric mixings appear to be essentially decoupled in the model. The LMA solar neutrino solution is obtained with a special form of M_R [11], which can be explained by the structure of the

Froggatt-Nielsen diagrams:

$$M_R = \begin{pmatrix} c^2\eta^2 & -b\epsilon\eta & a\eta \\ -b\epsilon\eta & \epsilon^2 & -\epsilon \\ a\eta & -\epsilon & 1 \end{pmatrix} \Lambda_R, \quad (4)$$

where the parameters ϵ and η are those introduced in Eq. (2) for the Dirac sector. The vanishing $2-3$ subdeterminant of M_R arises naturally if the Yukawa couplings are universal at the GUT scale. The new parameters a , b and c are undetermined but expected to be of $\mathcal{O}(1)$, since the first row and first column of M_R have been properly scaled by powers of the very small η parameter. As such, the right-handed Majorana mass matrix exhibits a very strong hierarchy.

Given the right-handed Majorana mass matrix above and $\delta_N = \delta'_N = 0$, the seesaw formula results in

$$\begin{aligned} M_\nu &= -M_N M_R^{-1} M_N^T \\ &= - \begin{pmatrix} 0 & \frac{1}{a-b}\epsilon & 0 \\ \frac{1}{a-b}\epsilon & \frac{b^2-c^2}{(a-b)^2}\epsilon^2 & \frac{b}{b-a}\epsilon \\ 0 & \frac{b}{b-a}\epsilon & 1 \end{pmatrix} m_U^2 / \Lambda_R. \end{aligned} \quad (5)$$

Note that the very strong hierarchy in M_R can nearly balance the large hierarchy in M_N to yield a rather mild mass hierarchy for the M_ν light neutrino mass matrix. In fact, if $M_R \propto M_N^T M_N$ were to hold, which has a texture similar to that in Eq. (4), the seesaw formula would yield a light neutrino mass matrix exactly proportional to the identity matrix resulting in a three-fold mass degeneracy. The author has argued in Ref. [7] that a normal hierarchy solution is much more stable than an inverted hierarchy solution for such type I seesaw models, and our results apply for this kind of solution. Barr has recently proposed more general possibilities which result in such a mild neutrino mass hierarchy [20].

The parameter Λ_R can be chosen real and to a large degree sets the scale for the atmospheric neutrino mixing mass squared difference. In most previous studies of the model, aside from that of leptogenesis, we chose the remaining three parameters, a , b and c , to be real. In order to determine the range of predictions for the neutrino mixing angles, we now allow all three of them to be complex.

III. RESULTS OF THE PARAMETER SEARCH

In order to carry out the search of the parameter space for a stable normal hierarchy solution, we shall require that the oscillation parameters determined by the model lie in the following presently allowed ranges at the 90% confidence level [1]-[4], [21]:

$$\begin{aligned}\Delta m_{32}^2 &= (1.9 - 3.0) \times 10^{-3} \text{ eV}^2, & \sin^2 \theta_{23} &= 0.36 - 0.64, \\ \Delta m_{21}^2 &= (7.4 - 8.5) \times 10^{-5} \text{ eV}^2, & \tan^2 \theta_{12} &= 0.33 - 0.50, \\ \Delta m_{31}^2 &\simeq \Delta m_{32}^2, & \sin^2 2\theta_{13} &\leq 0.16.\end{aligned}\tag{6}$$

The allowed variation in $\sin^2 \theta_{23}$ corresponds to the present bound of $\sin^2 2\theta_{23} \geq 0.92$ [1]. We find that the following bounds for the magnitudes of the input parameters in M_R cover the above experimentally allowed ranges:

$$|a| \leq 2.4, \quad |b| \leq 3.6, \quad |c| \leq 3.6,\tag{7}$$

where we have set $\Lambda_R = 2.85 \times 10^{14} \text{ GeV}$ as explained below. We then use Monte Carlo techniques to throw points in the complex a , b and c planes which uniformly cover the disks whose radii are indicated above.

It should be noted that in this paper, we shall neglect any running of the neutrino mass and mixing parameters from the GUT scale down to the low scales. This has become more or less standard procedure in the literature and is less susceptible to corrections when $\tan \beta$ is low, the neutrino mass hierarchy is normal, and the two low-lying neutrino mass eigenstates have nearly opposite CP -parities [22]. All three conditions hold in the model under consideration. In fact, we can use the convenient add-on program package for Mathematica called “REAP” provided by Antusch et al. [23] to test the assumption that the evolution effects are negligible for our case.

For this purpose, what is required in addition to the mass matrices in Eq. (2) is specification of the appropriate Higgs VEVs, $v_u \equiv \langle 5(\mathbf{10}_H) \rangle$ and $v_d \equiv \langle \bar{5}(\mathbf{10}_H) \rangle$ in Eq. (1), together with the two input scaling masses, m_U and m_D ; from these the corresponding Yukawa coupling matrices can be determined. Since $\langle H_u \rangle$ receives a contribution only from $\langle 5(\mathbf{10}_H) \rangle$, the 33 element of the Dirac matrix M_N is given by

$$(M_N)_{33} = m_U = (Y_N)_{33}v_u,\tag{8}$$

where Y_N is the Yukawa coupling matrix for the Dirac neutrino mass matrix and $v_u = v \sin \beta$ with $v = 174$ GeV as usual. On the other hand, $\langle H_d \rangle$ has two contributions from $\langle \bar{5}(\mathbf{10}_H) \rangle$ and $\langle \bar{5}(\mathbf{16}_H) \rangle$, but only the first contributes to the 33 element of the charged lepton mass matrix M_L ; hence

$$(M_L)_{33} = m_D = (Y_L)_{33} v_d \cos \gamma, \quad (9)$$

where Y_L is the Yukawa coupling matrix for the charged leptons and $\cos \gamma$ is the projection of H_d onto the VEV of $\langle \bar{5}(\mathbf{10}_H) \rangle \equiv v_d = v \cos \beta$. With $\tan \beta = v_u/v_d = 5$ as suggested earlier to provide a sufficiently lopsided charged lepton mass matrix, and the values for m_U and m_D in Eq. (3), we find that

$$\begin{aligned} Y_N &= 0.662(M_N/m_U), \\ Y'_L &\equiv Y_L \cos \gamma = 0.0293(M_L/m_D), \end{aligned} \quad (10)$$

where we have defined Y'_L as the effective charged lepton Yukawa coupling matrix due to the $\cos \gamma$ suppression. We assume that the VEVs, v_u and v_d , are held constant while Y_N and Y'_L evolve from the GUT scale to the weak scale according to the renormalization group equations.

By inserting this information into the REAP package of Antusch et al. [23], we can obtain the evolved results for the neutrino mixing parameters. We find for various test cases that the evolved mixing angles and phases are changed by less than 1% from their GUT scale values, while the light neutrino masses are reduced by 20%. The latter discrepancy can be corrected if we simply reduce the right-handed Majorana scaling factor Λ_R by 20% from 2.85×10^{14} GeV to 2.25×10^{14} GeV, with essentially no alteration in the mixing angles and phases. With this understanding of the role played by evolution of the Yukawa couplings, we simply ignore the evolution and proceed to use the GUT scale parameters given earlier.

Scatter plots are shown in Fig. 1 for the original choice of $\eta = 0.6 \times 10^{-5}$ and $\delta_N = \delta'_N = 0$. The atmospheric and solar neutrino mixing regions are shown in Figs. 1(a) and (b), where Δm_{32}^2 and Δm_{21}^2 are plotted against $\sin^2 2\theta_{atm} = 4|U_{\mu 3}|^2|U_{\tau 3}|^2$ and $\sin^2 2\theta_{sol} = 4|U_{e1}|^2|U_{e2}|^2$, respectively, the atmospheric and solar mixing angles in terms of the neutrino mixing matrix elements. For the atmospheric neutrino mixing, we observe from Fig. 1(a) that while Λ_R sets the scale for the mass squared difference, there is a spread of points for Δm_{32}^2 in the allowed interval $(1.9, 3.0) \times 10^{-3} \text{ eV}^2$; cf. Eq. (5). A value of $\Lambda_R = 2.85 \times 10^{14}$ GeV has been chosen, in order to center the allowed region predicted by the model on the experimentally

allowed region as determined by the Super Kamiokande data. For their best fit point of $\Delta m_{32}^2 = 2.4 \times 10^{-3} \text{ eV}^2$ and $\sin^2 2\theta_{23} = 1.00$, the model prefers a nearly maximal mixing angle of $\sin^2 2\theta_{23} \gtrsim 0.98$, in agreement with their finding. Note that the highest concentration of model points also occurs in this region surrounding their best fit point. For the solar neutrino mixing depicted in Fig. 1(b), we observe a nearly uniform spread in Δm_{21}^2 over the region allowed in Eq. (6) by the present data. On the other hand, for the solar mixing angle there is a slightly greater concentration of points toward the smaller allowed values for $\sin^2 2\theta_{sol}$.

Although it has been customary to present the neutrino mixing data in Δm^2 vs. $\sin^2 2\theta$ mixing planes as in Figs. 1(a) and (b), some authors [24] have suggested that $\sin^2 \theta$ is a more sensitive measure of the mixing angle, especially for angles close to a maximal mixing of 45° . Of particular interest is whether θ_{23} lies below 45° or above 45° , if the mixing is not exactly maximal. With a normal mass hierarchy as suggested by our model, the former signifies that the highest neutrino mass eigenstate corresponds more to a ν_τ flavor composition rather than to a ν_μ composition, while the opposite is true for the latter possibility. In Figs. 1(c)-(f) we also present results for (c) $\tan^2 \theta_{12}$, (d) $\sin^2 \theta_{13}$, (e) δ_{CP} , and (f) the baryon asymmetry, η_B , vs. $\sin^2 \theta_{23}$. We see from these plots that there is just a slight preference for values of $\sin^2 \theta_{23}$ greater than 0.5 than for those less than 0.5. Concerning the solar neutrino mixing angle distribution in Fig. 1(c), the full range of $0.33 \leq \tan^2 \theta_{12} \leq 0.50$ is populated, but values below 0.4 are slightly preferred to those above 0.4 in keeping with remarks made about Fig. 1(b). Nearly all the allowed points for $\sin^2 \theta_{13}$ in Fig. 1(d) are found to lie below 0.012 and above 1×10^{-5} , with those values above 0.001 most densely populated. Interestingly enough, the present best fits for $\sin^2 \theta_{13}$ are 0.006 and 0.004 from three-neutrino mixing analyses with all oscillation data considered [25]. The model seems to be rather insensitive to the leptonic CP-violating phase δ_{CP} in this more general search of the complex values for a , b and c , for the full range from -90° to 90° is essentially uniformly populated in Fig. 1(e). Finally we note that values for the baryon asymmetry in Fig. 1(f) are concentrated in the $10^{-13} - 10^{-12}$ range, which are much too small to explain the observed baryon asymmetry in the universe.

In Fig. 2, the corresponding scatter plots are presented for the choice $\eta = 1.1 \times 10^{-5}$, $\delta_N = -1.0 \times 10^{-5}$ and $\delta'_N = -1.5 \times 10^{-5}$. This latter choice has been made as a result of a protracted search, so as to maximize the calculated baryon asymmetry as we shall see, without spoiling the results in the quark sector. In the previous study reported in the last paper of reference

[16], the corresponding values taken were $\eta = 0.6 \times 10^{-5}$, $\delta_N = -0.65 \times 10^{-5}$ and $\delta'_N = -1.0 \times 10^{-5}$. But without altering the parameter, η , we observed a maximum of η_B which fell short of the presently observed baryon asymmetry.

The atmospheric neutrino mixing plane in Fig. 2(a) exhibits a somewhat stronger preference for lower values of Δm_{32}^2 than in Fig. 1(a), while the solar mixing angle distributions in Figs. 2(b) and (c) exhibit a slightly greater preference for smaller solar mixing angles. From Fig. 2(d) we see the upper bound on $\sin^2 \theta_{13}$ is predicted to lie lower than before in Fig. 1(d) and is now given by $\sin^2 \theta_{13} \lesssim 0.007$. The distribution is also somewhat more diffuse and less concentrated near the upper limit. Again no preferred values of the CP-violating phase δ_{CP} are observed in Fig. 2(e), but the baryon asymmetry is shifted to higher values in the broader range, 3×10^{-13} to 5×10^{-11} in Fig. 2(f).

The scatter plots presented in Figs. 1 and 2 were obtained by throwing 400,000 sets of points for the parameters a , b and c in the ranges given in Eq. (7) and demanding that the calculated mixing parameters lie in the experimental ranges quoted in Eq. (6). But the question arises whether more sparsely scattered points can be obtained outside the apparent boundaries. This is of special interest for the baryon asymmetry, where in fact one isolated point in Fig. 2(f) does show up with $\eta_B = 2.6 \times 10^{-10}$, well outside the major clustering but still below the observed value of 6.2×10^{-10} . Rather than throw 10 - 100 times as many points, we searched for M_R input parameters which favor larger values of η_B . We found such a region defined by constraining the parameters a , b and c to lie near or along their imaginary axes in the complex planes, still bounded by the magnitudes given in Eq. (7).

In Figs. 3(a) and (b), we present the scatter plots in the atmospheric and solar neutrino mixing planes obtained by throwing 100,000 sets of points for positive and negative imaginary values of a , b and c bounded by the magnitudes of Eq. (7), again for the new values of η , δ_N and δ'_N . While the solar mixing plane of Fig. 3(b) is very similar to that of Fig. 2(b), the atmospheric mixing plane in Fig. 3(a) is dramatically affected as the spread of points now lie along the arc shown. The upper branch corresponds to values of $\sin^2 \theta_{23} < 0.5$ and the lower branch to values of $\sin^2 \theta_{23} > 0.5$. The small secondary upper branch is obtained when $|c| < |a|$, while the major upper branch is found when $|c| > |a|$. Further insight into the restricted results are obtained from Figs. 3(c)-(f). Bands develop in all four plots of (c) $\tan^2 \theta_{12}$, (d) $\sin^2 \theta_{13}$, (e) δ_{CP} , and (f) η_B vs. $\sin^2 \theta_{23}$. One of the most striking results is that $\sin^2 \theta_{13}$ is now limited to the restricted range (0.0018, 0.0035). As seen in Fig. 3(f),

29 points have appeared in the $\eta_B > 1.0 \times 10^{-10}$ range.

In Fig. 4 similar plots for the mixing planes and distributions are shown, where 200,000 sets of points for imaginary values of a , b and c were thrown with the restriction $\eta_B \geq 1.0 \times 10^{-10}$ applied. In all 84 points survive this cut. We now see that the upper branch in the atmospheric neutrino mixing plane of Fig. 4(a) is essentially eliminated, for $\sin^2 \theta_{23} \gtrsim 0.47$ is required for most points to obtain such large values of η_B . The scatter points in the solar neutrino mixing plane is little affected aside from the density of points as seen in Fig. 4(b). The bands in Figs. 3(c), (d) and (e) become extremely narrow in Figs. 4(c), (d), and (e) when the cut $\eta_B \geq 1.0 \times 10^{-10}$ is imposed. A strong correlation arises between the solar mixing angle in $\tan^2 \theta_{12}$ and the atmospheric mixing angle in $\sin^2 \theta_{23}$; the larger the former, the smaller the latter. The upper bands in Figs. 4(d) and (e) are obtained when both parameters a and b have positive imaginary values and yield a positive Dirac phase δ_{CP} , while the lower bands arise from negative imaginary values for a and b . Note that for the restriction $\eta_B \geq 1.0 \times 10^{-10}$, the leptonic CP phase lies in the two ranges, $\pm(50^\circ, 80^\circ)$.

The distribution of points in η_B and $\sin^2 \theta_{23}$ which survive the cut of $\eta_B \geq 1.0 \times 10^{-10}$ is shown in Fig. 4(f). Several points with $\eta_B \simeq 6.0 \times 10^{-10}$ are observed to be clustered around $\sin^2 \theta_{23} \simeq 0.6$. For these few points, values of $c \sim \pm a$ seem to be preferred. This suggested that we construct scatter plots with all three parameters, a , b and c taken to be imaginary with the restriction $c = a$. The corresponding plots are shown in Fig. 5, where 100,000 sets of points are thrown and 381 points survive. It is rather remarkable that the atmospheric neutrino mixing plane in Fig. 5(a) is restricted to a short arc centered at $\Delta m_{32}^2 = 2.45 \times 10^{-3} \text{ eV}^2$ and with $\sin^2 2\theta_{\text{atm}}$ lying in the range (0.985, 0.995), as $0.45 \leq \sin^2 \theta_{23} \leq 0.55$ with $2.30 \times 10^{-3} \leq \Delta m_{32}^2 \leq 2.65 \times 10^{-3} \text{ eV}^2$ for our choice of Λ_R . The solar mixing plane in Fig. 5(b) is also somewhat truncated at the lower end of the spectrum as now $\sin^2 2\theta_{\text{sol}} \gtrsim 0.80$. The bands in Figs. 5(c)-(e) are similar to those in Fig. 4(c)-(e) but again somewhat truncated by the maximum value of θ_{23} . The relevant values of $\sin^2 \theta_{13}$ now lie in the interval (0.0020, 0.0031). The CP phase is bounded by $\pm(60^\circ, 86^\circ)$ in Fig. 5(f).

With the strong correlation of the mixing angles noted above, η_B is now directly related to the mixing angle θ_{23} in Fig. 5(f), as the random scattering in Fig. 4(f) has disappeared. The observed baryon asymmetry value of 6.2×10^{-10} is obtained for $\sin^2 \theta_{23} \simeq 0.55$, which implies $\tan^2 \theta_{12} \simeq 0.38$, $\sin^2 \theta_{13} \simeq 0.0021$ and $\delta_{CP} \simeq \pm 60^\circ$. For this case the sum of θ_{12} and the Cabibbo angle is given by $\theta_C + \theta_{12} = 44.8^\circ$, very close to the value of 45° which

is referred to as quark-lepton complementarity in the literature [26]. On the other hand, maximal atmospheric neutrino mixing with $\sin^2 \theta_{23} = 0.5$ corresponds to $\tan^2 \theta_{12} = 0.44$, $\sin^2 \theta_{13} \simeq 0.0024$, $\delta_{CP} = \pm 75^\circ$, and $\eta_B = 3.8 \times 10^{-10}$.

As an example of a complete solution, we present the results for a special case which arises for the choice of right-handed Majorana neutrino parameters: $a = 0.5828i$, $b = 1.7670i$, $c = 0.5828i$ with $\Lambda_R = 2.85 \times 10^{14}$ GeV, $\eta = 1.1 \times 10^{-5}$, $\delta_N = -1.0 \times 10^{-5}$, and $\delta'_N = -1.5 \times 10^{-5}$. One obtains $\eta_B = 6.2 \times 10^{-10}$ with the following mixing parameters

$$\begin{aligned} \Delta m_{32}^2 &= 2.30 \times 10^{-3} \text{ eV}^2, & \sin^2 \theta_{23} &= 0.550, \\ \Delta m_{21}^2 &= 7.71 \times 10^{-5} \text{ eV}^2, & \tan^2 \theta_{12} &= 0.388, \\ \sin^2 \theta_{13} &= 0.0022, & \delta_{CP} &= 63^\circ, \\ \chi_1 &= -55.3^\circ, & \chi_2 &= 31.8^\circ, \end{aligned} \tag{11}$$

where χ_1 and χ_2 are the Majorana phases in the Majorana phase matrix, $\Phi = \text{diag}(\exp i\chi_1, \exp i\chi_2, 1)$. For this case, $m_3 = 48.9$ meV, $m_2 = 9.30$ meV, $m_1 = 3.05$ meV, $M_3 = 2.91 \times 10^{14}$ GeV, $M_1 \sim M_2 \sim 5.40 \times 10^8$ GeV, $M_2 - M_1 = 1.06 \times 10^3$ GeV, and $\Gamma_1 = 2.07 \times 10^3$ GeV where Γ_1 is the width of the lightest right-handed state.

Further study reveals that the narrow band structures in Fig. 5, obtained with a , b and c pure imaginary and $c = a$, arise because b is limited to the very narrow ranges, $b = \pm(1.7 \text{ to } 2.1)i$, for all 381 points which satisfy the mixing parameter constraints imposed in Eq. (6). On the other hand, the ratio a/b varies in the range $a/b = (0.33 \text{ to } 0.53)$ along each band as $\sin^2 \theta_{23}$ decreases from 0.55 to 0.45. The pair of slightly displaced bands in Fig. 5(d) is associated with the choices of positive or negative imaginary values for a and b . Clearly the imposition of these restrictions for the a , b , c parameter set has greatly enhanced the probability that the baryon asymmetry will lie in or near to its observed value. This makes for a rather compelling scenario within the model.

The question arises as to how likely is it that such restricted values should apply for the Majorana mass parameters. It is easy to see from the Froggatt-Nielsen diagrams for the Majorana mass matrix that if only one Higgs VEV is responsible for breaking lepton number, by the $U(1) \times Z_2 \times Z_2$ family symmetry of the model only one diagram will contribute to each matrix element, the structure of M_R will be purely geometrical and its determinant will vanish, cf. Ref. [11]. With $b \neq c = a$, only one diagram contributes to each of the 11, 13, and 31 matrix elements, while two or more diagrams will be required for the 12 and 21

elements. This is the simplest possibility for a nonvanishing determinant, as required for the seesaw mechanism. The fact that all three parameters are purely imaginary makes for a maximum CP violation in the right-handed Majorana mass matrix as all other parameters are real.

To understand the apparent difficulty in reaching values in the observed range of $\eta_B \simeq 6.2 \times 10^{-10}$, we note the following. The scenario of resonant leptogenesis [27] arises naturally in the model, for the two heavy right-handed Majorana neutrinos have nearly equal masses and nearly opposite CP-parity. However, one must impose the condition that the mass difference of these two heavy Majorana states be at least as large as the half-width of either state for the resonance formula to make sense. This forced us to raise the magnitudes of η , δ_N and δ'_N in the Dirac neutrino mass matrix. For smaller values of these parameters than those chosen in the relevant figures, fewer points reach the 10^{-10} range of η_B , as the range of $\sin^2 \theta_{23}$ is shifted lower with more points occurring below 0.50 than above 0.50. It is interesting that in going from the set of matrices with the original choice of η , δ_N and δ'_N in Fig. 1 to the new choice of values in Figs. 2 - 5, the V_{us} mixing parameter in the quark mixing matrix is raised from 0.2220 to 0.2240, in better keeping with the new observed value which is preferred for unitarity reasons. The one negative effect in making this change is that the up quark mass is raised from 3.5 MeV to 5.5 MeV after evolution from the GUT scale, which is above the preferred range.

While the condition for thermal resonant leptogenesis is easily satisfied for such right-handed Majorana masses as in the example given above, the overproduction of gravitinos in the early universe is a problem in the supergravity scenario of SUSY breaking; this can be alleviated if the SUSY breaking occurs via the gauge-mediated scenario [28]. As illustrated in Ref. [16], this problem can be completely avoided and satisfactory leptogenesis and baryon asymmetry obtained, if the model is expanded to include three additional intermediate mass scale singlets which lead to a double seesaw mechanism. However, with this expanded seesaw mechanism many more parameters are introduced, and the model becomes much less predictive.

IV. CONCLUDING REMARKS

From the above results we can conclude that the model with a normal mass hierarchy can easily fit the presently observed neutrino mixing data. As originally proposed, eight of the twelve model parameters have been fixed by the quark and lepton masses and quark mixing data, while the remaining four (three complex and one real) parameters of the right-handed Majorana mass matrix are varied. The real Λ_R parameter centers the Δm_{32}^2 model spectrum on the observed 90% confidence level interval given in Eq. (6). For the best fit point of $\Delta m_{32}^2 = 2.4 \times 10^{-3} \text{ eV}^2$, the predicted atmospheric neutrino mixing angle is nearly maximal, corresponding to $\sin^2 2\theta_{23} \gtrsim 0.98$ in agreement with the observed best fit value of 1.00. No such preference for a particular value of $\tan^2 \theta_{12}$ in the allowed range is found. The predicted values for $\sin^2 \theta_{13}$ are of special interest. There we found a range of $1 \times 10^{-5} \lesssim \sin^2 \theta_{13} \lesssim 0.01$ which lies noticeably lower than that predicted by most other models where values very close to the upper bound of 0.04 are more generally expected [29]. This is true not only for the nearly conserved $L_e - L_\mu - L_\tau$ models, but also for the $SO(10)$ models with symmetric $\mathbf{126}_H$ and $\overline{\mathbf{126}}_H$ Higgs representations. The lower values predicted in our model have relevance for the future study of neutrino oscillations with reactor beams. If $\bar{\nu}_e$ disappearance is observed very close to the present CHOOZ bound by the next generation reactor experiments, the $SO(10)$ model under consideration will be ruled out. On the other hand, it is interesting to note that if future reactor experiments do not see some $\bar{\nu}_e$ disappearance, the model predicts it will certainly be seen with superbeam and/or neutrino factory experiments. While there remains much interest in determining the Dirac phase δ_{CP} for CP violation, it is rather surprising that the model is able to accommodate almost any value.

With the original Dirac neutrino mass parameters, the resonance leptogenesis inherent in the model generated a baryon asymmetry which falls more than two orders of magnitude short of the observed value. In an effort to increase the effect, the original very small η parameter was adjusted and two new equally small parameters, δ_N and δ'_N , were added to the Dirac neutrino mass matrix. This helped to recover two missing orders of magnitude for η_B , provided the three complex parameters in the right-handed Majorana mass matrix were chosen very near to or on their imaginary axes. By selecting only those points which satisfied the observed neutrino mixing results and for which $\eta_B \gtrsim 1.0 \times 10^{-10}$, we observed that the mixing angles lie along very narrow bands.

These bands were further dramatically tightened by choosing not only a , b and c purely imaginary, but restricting c to be equal to a . For this situation a limited range of $0.45 \leq \sin^2 \theta_{23} \leq 0.55$ was found over which $\tan^2 \theta_{12}$ falls from 0.50 to 0.38, $\sin^2 \theta_{13}$ varies from 0.0031 to 0.0020, and the Dirac CP phase varies from $\pm(85^\circ \text{ to } 60^\circ)$. On the other hand, a narrow band also developed for the baryon asymmetry due to the strong mixing angle and CP phase correlations, as it rises from $(2.7 \text{ to } 6.3) \times 10^{-10}$ with increasing $\sin^2 \theta_{23}$. The appearance of such narrow bands is directly related to the very narrow acceptable range for b , while the ratio a/b varies along the length of each band. We argued that the $c = a$ restriction can be understood in terms of one Froggatt-Nielsen diagram for each of the 11, 13, and 31 matrix elements of M_R , while two such diagrams can contribute to the 12 and 21 elements. All these results are of considerable interest and will severely test the model in the future.

Since the light neutrino mass spectrum has a normal hierarchy, the model predicts no neutrinoless double beta decay should be observed in the near future. In fact, for all choices of the model parameters which lead to acceptable ranges for the mixing parameters of Eq. (6), we find the effective mass is $m_{\beta\beta} \sim 0.4 \times 10^{-3} \text{ eV}$ [7], three orders of magnitude below the present bound [30].

In conclusion, we address briefly the issue of lepton flavor violation in the decay process $\mu \rightarrow e + \gamma$. Jankowski and Maybury [12] have studied this particular class of $SO(10)$ models with lopsided charged lepton mass matrices in order to determine the expected branching ratio for the above decay, under the assumption that the supersymmetric grand unified model breaks directly to the constrained minimal supersymmetric standard model. Given the combined constraints on the CMSSM parameters from direct searches and from the WMAP satellite observations [17, 31], they find that for a low value of $\tan \beta \simeq 5$ preferred by the model, the branching ratio should be of $\mathcal{O}(10^{-12})$ and very close to the present upper limit of 1.2×10^{-11} [32]. Hence the $\mu \rightarrow e + \gamma$ decay should be observed in the new MEG experiment [13] which is expected to start taking data in 2006. This prediction is based on the slepton masses being in the 125 - 150 GeV range, while the neutralino masses are around 300 - 500 GeV. These ranges are also favored in CMSSM models by the recent study of the best chi-squared fits to all the data with $\tan \beta \simeq 10$ by Ellis et al. [33]. On the other hand, minimal $SO(10)$ models leading to symmetric or antisymmetric mass matrix elements favor a smaller lepton-violating branching ratio of $\mathcal{O}(10^{-13})$ or less [34]. The

coming MEG experiment which is expected to be sensitive down to the 10^{-14} branching ratio level may thus be able to rule out one of the two classes of minimal $SO(10)$ models before the new reactor experiments can be launched.

The author thanks Uli Haisch and Enrico Lunghi for their help with the scatter plots. The author also thanks the Theory Group at Fermilab for its kind hospitality. Fermilab is operated by Universities Research Association Inc. under contract No. DE-AC02-76CH03000 with the Department of Energy.

-
- [1] Y. Ashie et al. (Super-Kamiokande Collab.), Phys. Rev. Lett. **93**, 101801 (2004); Y. Ashie et al. (Super-Kamiokande Collab.), hep-ex/0501064.
 - [2] S.N. Ahmed et al. (SNO Collab.), Phys. Rev. Lett. **92**, 181301 (2004); B.T. Cleveland et al. (Homestake Collab.), Astrophys. J. **496**, 505 (1998); J.N. Abdurashitov et al. (SAGE Collab.), Phys. Rev. Lett. **83**, 4686 (1999); W. Hampel et al. (GALLEX Collab.), Phys. Lett. B **447**, 127 (1999); M. Altmann et al. (GNO Collab.), Phys. Lett. B **490**, 16 (2000).
 - [3] M.H. Ahn et al. (K2K Collab.), Phys. Rev. Lett. **90**, 041801 (2003).
 - [4] K. Eguchi et al. (KamLAND Collab.), Phys. Rev. Lett. **90**, 021802 (2003); T. Araki et al. (KamLAND Collab.), Phys. Rev. Lett. **94**, 081801 (2005).
 - [5] For several reviews, see S.F. King, Rept. Prog. Phys. **67**, 107 (2004); G. Altarelli and F. Feruglio, New J. Phys. **6**, 106 (2004); R.N. Mohapatra, New J. Phys. **6**, 82 (2004); S.M. Barr and I. Dorsner, Nucl. Phys. B **585**, 79 (2000).
 - [6] For the earliest and some of the latest such models cf. S. Petcov, Phys.Lett. B **110**, 245 (1982); R. Barbieri, L. Hall, D. Smith, A. Strumia, and N. Weiner, JHEP **9812**, 017 (1998); A. Joshipura and S. Rindani, Eur. Phys. J. C **14**, 85 (2000); R.N. Mohapatra, A. Perez-Lorenzana, and C. de S. Pires, Phys. Lett. B **474**, 355 (2000); S.T. Petcov and W. Rodejohann, Phys. Rev. D **71**, 073002 (2005); W. Grimus and L. Lavoura, J. Phys. G **31**, 683 (2005).
 - [7] C.H. Albright, Phys. Lett. B **599**, 285 (2004).
 - [8] K.S. Babu and R.N. Mohapatra, Phys. Rev. Lett. **70**, 2845 (1993); Mu-C. Chen and K.T. Mahanthappa, Phys. Rev. D **62**, 113007 (2000); T. Fukuyama and N. Okada, JHEP **0211**, 011 (2002); H.S. Goh, R.N. Mohapatra, and S.P. Ng, Phys. Lett. B **570**, 215 (2003); M. Bando

- and M. Obara, Prog. Theor. Phys. **109**, 995 (2003); G.G. Ross and L. Velasco-Sevilla, Nucl. Phys. B **653**, 3 (2003); C.S. Aulakh, B. Bajc, A. Melfo, G. Senjanovic, and F. Vissani, Phys. Lett. B **588**, 196 (2004); M. Bando, S. Kaneko, M. Obara, and M. Tanimoto, Phys. Lett. B **580**, 229 (2004); B. Dutta, Y. Mimura, and R.N. Mohapatra, Phys. Lett. B **603**, 35 (2004).
- [9] C.H. Albright and S.M. Barr, Phys. Rev. D **58**, 013002 (1998); K.S. Babu, J.C. Pati, and F. Wilczek, Nucl. Phys. B **566**, 33 (2000); T. Blazek, S. Raby, and K. Tobe, Phys. Rev. D **62**, 055001 (2000); R. Kitano and Y. Mimura, Phys. Rev. D **63**, 016008 (2001); Z. Berezhiani and A. Rossi, Nucl. Phys. B **594**, 113 (2001).
- [10] C.H. Albright, K.S. Babu, and S.M. Barr, Phys. Rev. Lett. **81**, 1167 (1998).
- [11] C.H. Albright and S.M. Barr, Phys. Rev. Lett. **85**, 244 (2000); Phys. Rev. D **62**, 093008 (2000); Phys. Rev. D **64**, 073010 (2001).
- [12] E. Jankowski and D.W. Maybury, Phys. Rev. D **70**, 035004 (2004).
- [13] T. Mori (MEG Collab.), talk presented at the SUSY 2004 Conference, Tsukuba, Japan (2004).
- [14] S.M. Barr and S. Raby, Phys. Rev. Lett. **79**, 4748 (1997).
- [15] C.D. Froggatt and H.B. Nielsen, Nucl. Phys. B **147**, 277 (1979).
- [16] C.H. Albright and S.M. Barr, Phys. Rev. D **69**, 073010 (2004); Phys. Rev. D **70**, 033013 (2004).
- [17] D.N. Spergel et al., Astrophys.J. Suppl. **148**, 175 (2003).
- [18] For an updated list of the input parameters, cf. Ref. [16].
- [19] P. Minkowski, Phys. Lett. B **67**, 421 (1977); T. Yanagida, in *Proceedings of the Workshop on Unified Theory and the Baryon Number of the Universe*, Tsukuba, Japan, 1979, p. 95; M. Gell-Mann, P. Ramond, and R. Slansky, in *Supergravity*, (P. van Nieuwenhuizen and D.Z. Freedman, eds.), North Holland, Amsterdam, 1979, p. 315; S.L. Glashow, in *Proceedings of the 1979 Cargese Summer Institute on Quarks and Leptons*, (M. Levy, J.-L. Basdevant, D. Speiser, J. Weyers, R. Gastmans, and M. Jacob, eds.), Plenum Press, New York, 1980, p. 687; R.N. Mohapatra and G. Senjanovic, Phys. Rev. Lett. **44**, 912 (1980); J. Schechter and J.W.F. Valle, Phys. Rev. D **22**, 2227 (1980).
- [20] S.M. Barr, hep-ph/0502129.
- [21] M. Apollonio et al. (CHOOZ Collab.), Phys. Lett. B **466**, 415 (1999); F. Boehm et al. (Palo Verde Collab.), Phys. Rev. D **64**, 112001 (2001).
- [22] P.H. Chankowski and S. Pokorski, Int. J. Mod. Phys. A **17**, 575 (2002).

- [23] S. Antusch, J. Kersten, M. Lindner, M. Ratz, and M.A. Schmidt, JHEP **0503**, 024 (2005).
- [24] O. Mena and S. Parke, Phys. Rev. D **69**, 117301 (2004).
- [25] M. Maltoni, T. Schwetz, M.A. Tortola, and J.W.F. Valle, Phys. Rev. D **68**, 113010 (2003); S. Goswami and A.Yu. Smirnov, hep-ph/0411359.
- [26] M. Raidal, Phys. Rev. Lett. **93**, 161801 (2004); H. Minakata and A. Yu. Smirnov, Phys. Rev. D **70**, 073009 (2004).
- [27] M. Fukugita and T. Yanagida, Phys. Lett. B **174**, 45 (1986); M. Flanz, E.A. Paschos, U. Sarkar, and J. Weiss, Phys. Lett. B **389**, 693 (1996); L. Covi and E. Roulet, *ibid.* **399**, 113 (1997).
- [28] M. Kawasaki, K. Kohri, and T. Morioi, astro-ph/0402490.
- [29] Brief summaries of model predictions for θ_{13} can be found in C.H. Albright, Int. J. Mod. Phys. A **18**, 3947 (2003); M.-C. Chen and K.T. Mahanthappa, Int. J. Mod. Phys. A **18**, 5819 (2003).
- [30] C. Aalseth et al., Summary report of the APS Multidivisional Neutrino Study, hep-ph/0412300.
- [31] C.L. Bennett et al. (WMAP Collab.), Astrophys. J. Suppl. **148**, 1 (2003).
- [32] M.L. Brooks et al. (MEGA Collab.), Phys. Rev. Lett. **83**, 1521 (1999).
- [33] J. Ellis, S. Heinemeyer, K.A. Olive, and G. Weiglein, JHEP **0502**, 013 (2005); J. Ellis, K.A. Olive, Y. Santoso, and V.C. Spanos, hep-ph/0502001.
- [34] A. Masiero, S.K. Vempati, and O. Vives, New J. Phys. **6**, 202 (2004); M.-C. Chen and K.T. Mahanthappa, Phys. Rev. D **70**, 113013 (2004); I. Masina and C.A. Savoy, hep-ph/0501166.

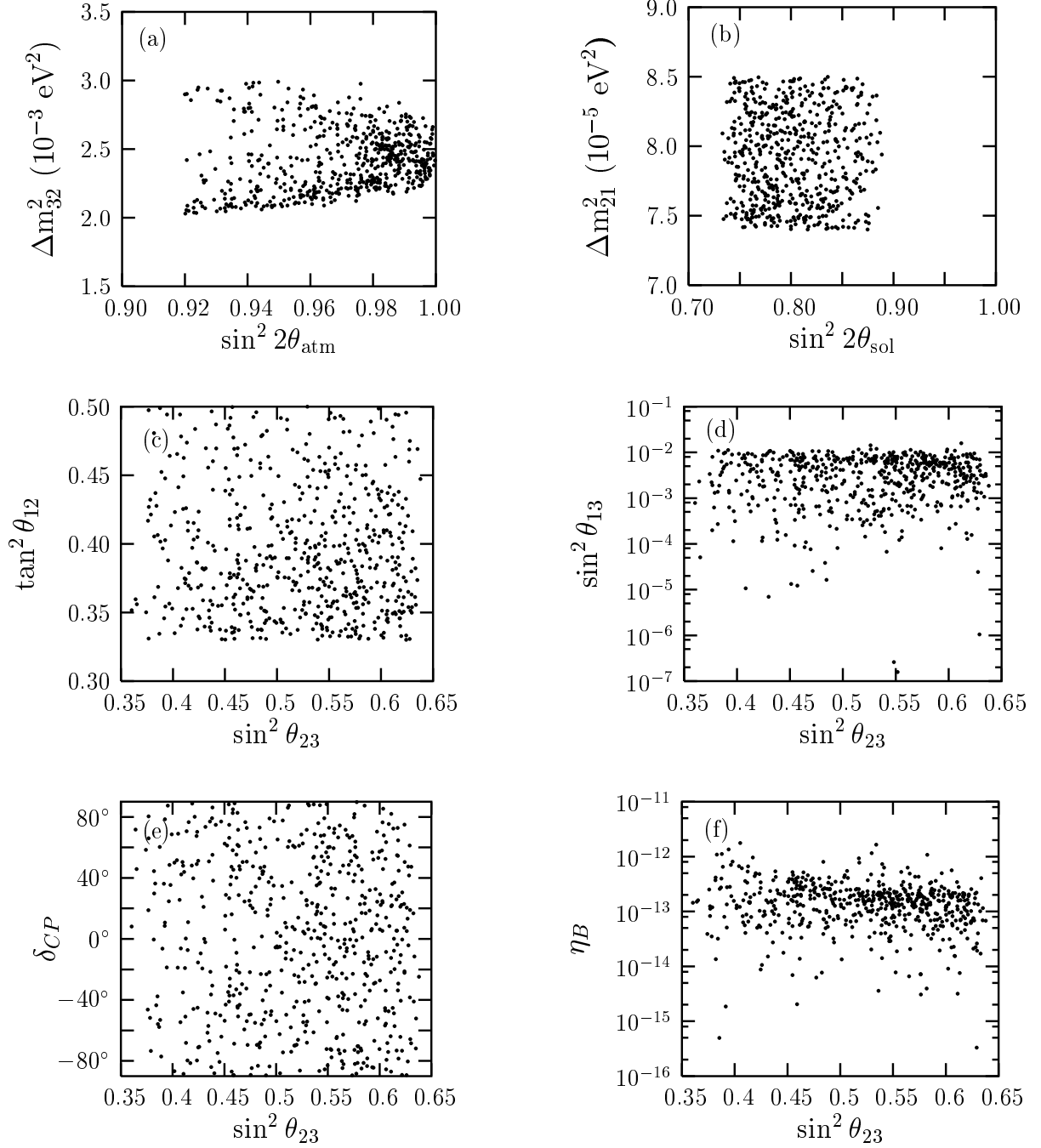


Fig. 1. Plots of (a) Δm_{32}^2 vs. $\sin^2 2\theta_{23}$, (b) Δm_{21}^2 vs $\sin^2 2\theta_{12}$; and (c) $\tan^2 \theta_{12}$, (d) $\sin^2 \theta_{12}$, (e) δ_{CP} , and (f) η_B vs. $\sin^2 \theta_{23}$ for the original choice of $\eta = 0.6 \times 10^{-5}$ and $\delta_N = \delta'_N = 0$ in the Dirac neutrino mass matrix. A value of $\Lambda_R = 2.85 \times 10^{14} \text{ GeV}$ applies for all figures.

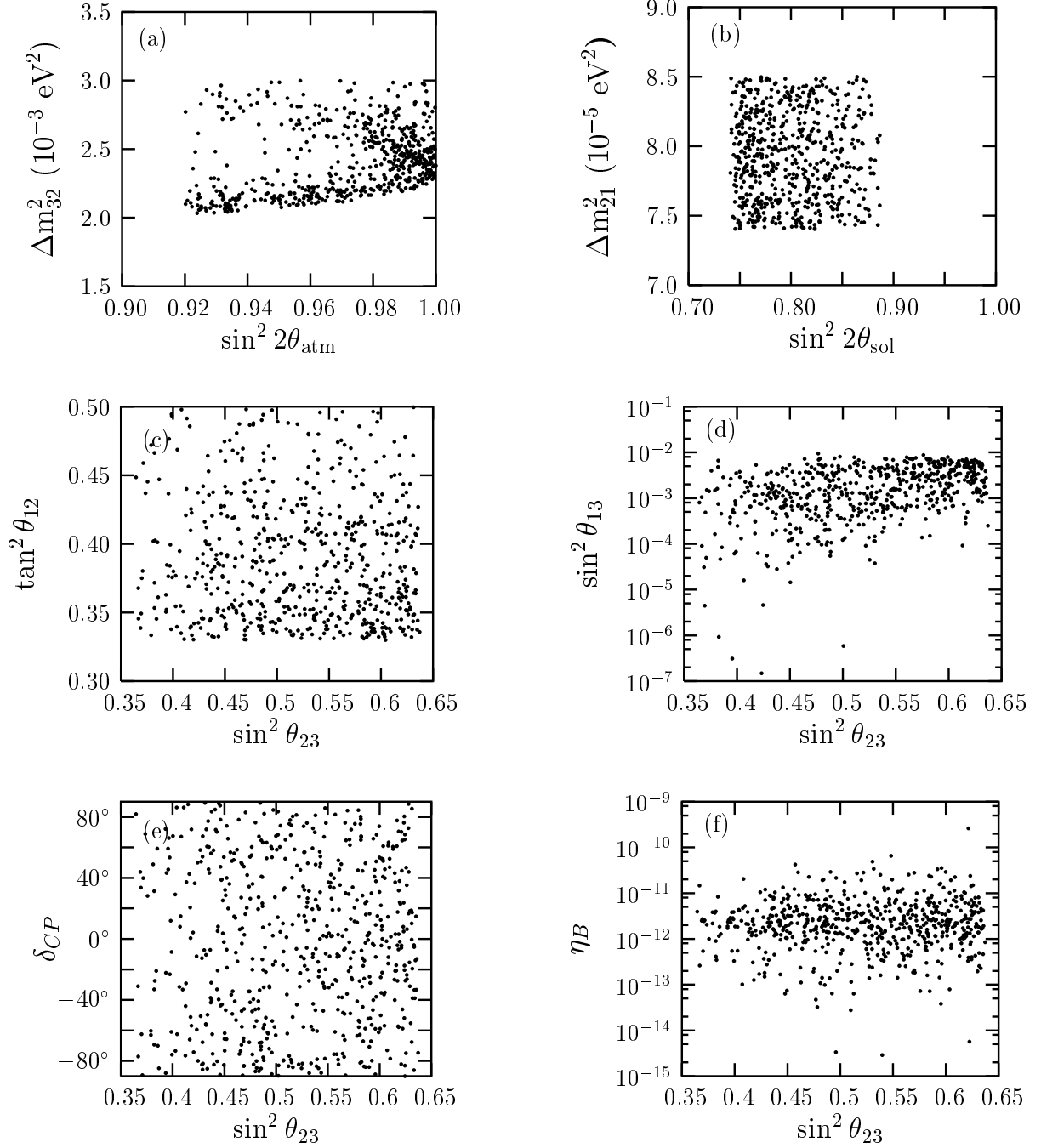


Fig. 2. Plots of (a) Δm_{32}^2 vs. $\sin^2 2\theta_{23}$, (b) Δm_{21}^2 vs. $\sin^2 2\theta_{12}$; and (c) $\tan^2 \theta_{12}$, (d) $\sin^2 \theta_{12}$, (e) δ_{CP} , and (f) η_B vs. $\sin^2 \theta_{23}$ for the choice of $\eta = 1.1 \times 10^{-5}$, $\delta_N = -1.0 \times 10^{-5}$, and $\delta'_N = -1.5 \times 10^{-5}$ in the Dirac neutrino mass matrix.

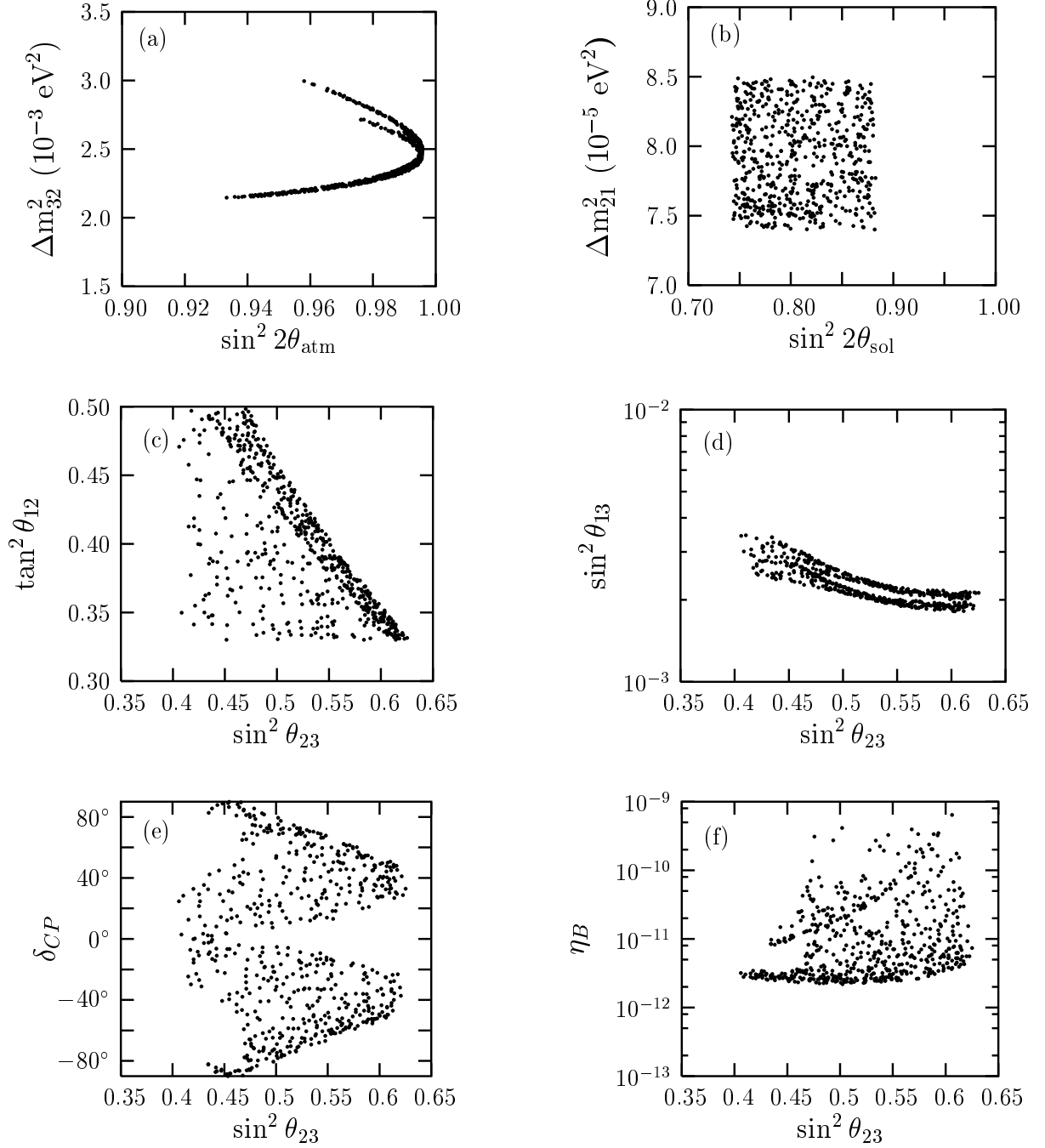


Fig. 3. Plots of (a) Δm_{32}^2 vs. $\sin^2 2\theta_{23}$, (b) Δm_{21}^2 vs $\sin^2 2\theta_{12}$; and (c) $\tan^2 \theta_{12}$, (d) $\sin^2 \theta_{12}$, (e) δ_{CP} , and (f) η_B vs. $\sin^2 \theta_{23}$ for the choice of $\eta = 1.1 \times 10^{-5}$, $\delta_N = -1.0 \times 10^{-5}$, and $\delta'_N = -1.5 \times 10^{-5}$ in the Dirac neutrino mass matrix. The parameters a , b , and c in the right-handed Majorana mass matrix are constrained to lie along their imaginary axes.

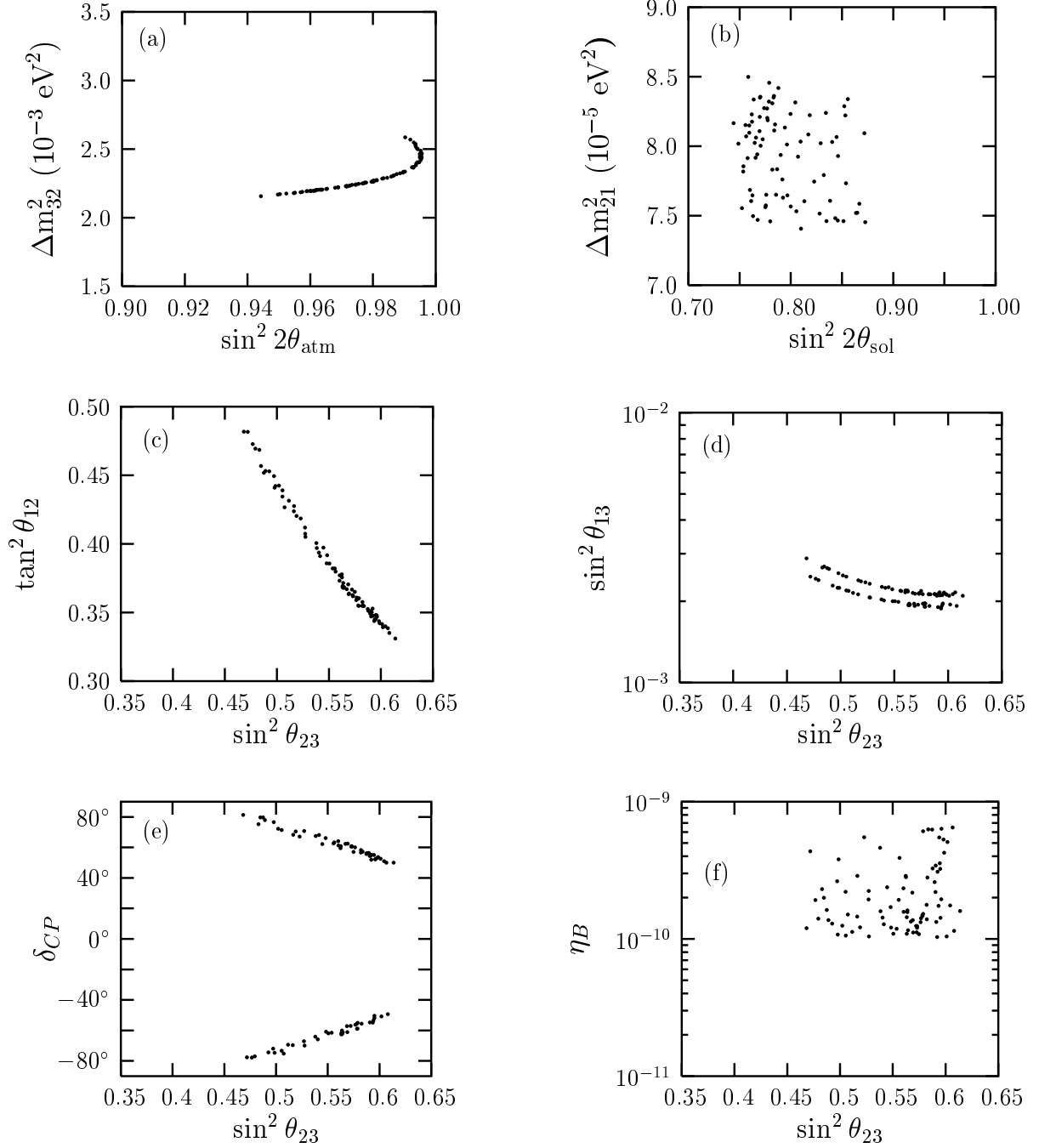


Fig. 4. Plots of (a) Δm_{32}^2 vs. $\sin^2 2\theta_{23}$, (b) Δm_{21}^2 vs $\sin^2 2\theta_{12}$; and (c) $\tan^2 \theta_{12}$, (d) $\sin^2 \theta_{12}$, (e) δ_{CP} , and (f) η_B vs. $\sin^2 \theta_{23}$ for the choice of $\eta = 1.1 \times 10^{-5}$, $\delta_N = -1.0 \times 10^{-5}$, and $\delta'_N = -1.5 \times 10^{-5}$ in the Dirac neutrino mass matrix. The parameters a , b , and c in the right-handed Majorana mass matrix are constrained to lie along their imaginary axes. The condition $\eta_B \geq 10^{-10}$ is imposed.

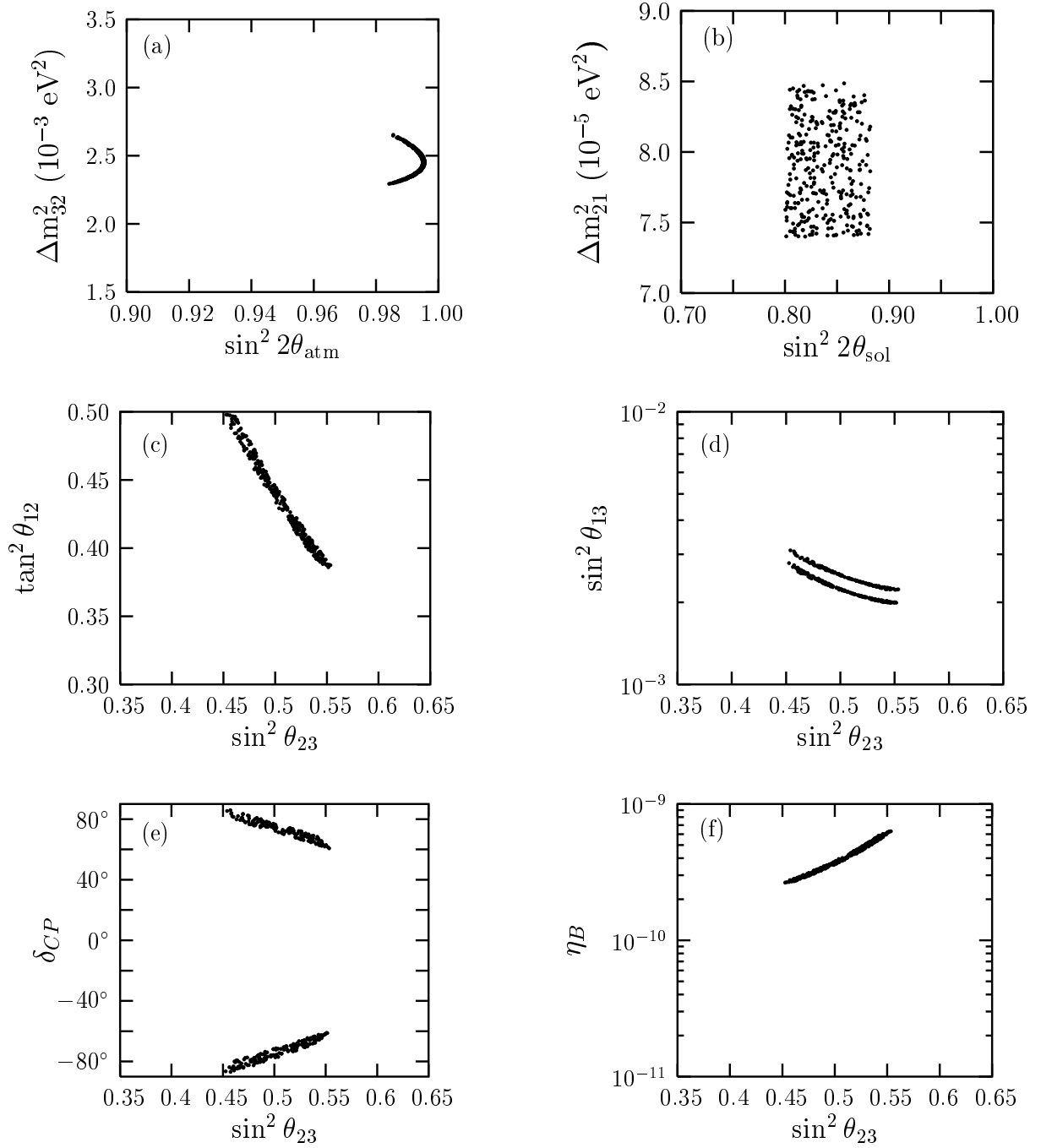


Fig. 5. Plots of (a) Δm_{32}^2 vs. $\sin^2 2\theta_{23}$, (b) Δm_{21}^2 vs $\sin^2 2\theta_{12}$, and (c) $\tan^2 \theta_{12}$, (d) $\sin^2 \theta_{12}$, (e) δ_{CP} , and (f) η_B vs. $\sin^2 \theta_{23}$ for the choice of $\eta = 1.1 \times 10^{-5}$, $\delta_N = -1.0 \times 10^{-5}$, and $\delta'_N = -1.5 \times 10^{-5}$. Here the parameters a , b and c are constrained to lie along their imaginary axes with $c = a$.